Nature of Interaction between Basic Fibroblast Growth Factor and the Antiangiogenic Drug 7,7-(Carbonyl-Bis[Imino-*N*-Methyl-4,2-Pyrrolecarbonylimino[*N*-Methyl-4,2-Pyrrole]-Carbonylimino])-Bis-(1,3-Naphtalene Disulfonate). II. Removal of Polar Interactions Affects Protein Folding

Moreno Zamai,*† Chithra Hariharan,* Dina Pines,* Michal Safran,‡ Avner Yayon,‡ Valeria R. Caiolfa,§ Rivka Cohen-Luria,* Ehud Pines,* and Abraham H. Parola*

*Department of Chemistry, Ben Gurion University of The Negev, Beer-Sheva, 84105, Israel; †Oncology, Department of Biology, Discovery Research, Pharmacia Corporation, via Pasteur 10, 20014 Nerviano, Milan, Italy; ‡Department of Molecular Cell Biology, Weizmann Institute of Science, Rehovot, Israel; and §San Raffaele Scientific Institute, via Olgettina, 58 20132 Milan, Italy

ABSTRACT Fibroblast growth factor-2 (basic FGF), a potent inducer of angiogenesis, and the naphthalene sulfonic distamycin A derivative, 7,7-(carbonyl-bis[imino-*N*-methyl-4,2-pyrrolecarbonylimino[*N*-methyl-4,2-pyrrole]-carbonylimino])-bis-(1,3-naphtalene disulfonate) (PNU145156E), which exhibits in vivo antiangiogenic activity, form a tight reversible (1:1) complex. PNU145156E binds to the heparin and the selenate-binding sites on bFGF. The *cis* bFGF-heparin (2:1) complex, essential for the activation of the angiogenic process, is thus prevented. The nature of the forces involved in bFGF: PNU145156E complex, using the wild-type and the K128Q, K138Q, K134Q, and K128Q-K138Q point mutated bFGFs was sought. Based on thermodynamic analysis of the complexation constants, protein temperature stability profiles by ultraviolet absorption, circular dichroism measurements, fluorescence Förster energy-transfer, and anisotropy studies, in harmony with the published x-ray crystallographic structure, the following molecular interactions are proposed: reduced coulombic interactions, hence loosening of the complex by the removal of charged polar groups from the bFGF-heparin binding cleft resulted in decreased binding constants and in a change in the binding mode from polar to nonpolar. Concomitantly, upon mutation, the protein was rendered more compact, less flexible, and less aqueously exposed compared with the wild type. These were further pronounced with the double mutant: weaker dominantly nonpolar protein-drug interactions were accompanied by conspicuous folding. With heparin, however, wild-type bFGF forms a tighter complex with a more compact structure.

INTRODUCTION

Angiogenesis, the growth of new blood vessels, results from a series of molecular events that are regulated by stimulators and inhibitors (Klagsbrun and D'Amore, 1991). This process is fundamental in the development, progression, and metastatic spread of solid tumors (Folkman, 1971, 1985; Folkman and Klagsbrun, 1987). A variety of tumor-induced angiogenesis factors have been identified and are known to have widespread effect on different steps of angiogenesis (Gullino, 1978; Blood and Zetter, 1990; Liotta et al., 1991). One important class of angiogenesis-promoting proteins is the heparin-binding growth factors characterized by their high affinity to heparan sulfate proteoglycans. Human fibroblast growth factors (FGFs) are the most important of them (Burgess and Maciag, 1989; Biasoli et al., 1993; Presta et al., 1994). X-ray crystallographic studies show that FGFs take up a β-trefoil structure with a cavity in its center surrounded by hydrophobic residues (Eriksson et al., 1993). This cavity that consists of three copies of basic four stranded antiparallel β-sheets is characteristic to the family of β-trefoil proteins. The same hydrophobic residues are conserved in all of them, suggesting that the hydrophobic interaction in the cavity play an important role in maintaining the overall structure (Ogura et al., 1999). Chemical and site-directed mutagenesis studies on basic FGF (bFGF) supported by x-ray crystallography have identified separate functional domains for heparin and receptor binding (Baird et al., 1988; Zhu et al., 1990, 1995; Eriksson et al., 1993; Li et al., 1994; Springer et al., 1994; Thompson et al., 1994). Various roles for the interaction of heparin and heparan sulfate proteoglycans with bFGF have been proposed, including stabilization of the protein, protection from proteolytic degradation, extracellular storage, and most importantly, mediating the binding of bFGF to its cell surface tyrosine kinase receptor (Yayon et al., 1991; Fernig and Gallagher, 1994; Lindahl et al., 1994; Ornitz et al., 1995; Faham et al., 1996; Venkataraman et al., 1996; Digabriele et al., 1998; Plotnikov et al., 1999).

Studies on the activation of FGFs by heparin using several model compounds (e.g., tetrasaccharide, hexasaccharide, myoinositol hexasulphate (MIHS)) showed that the binding to these analogs greatly increases the definition of those regions of the protein recognized by the cell surface tyrosine kinase receptors that trigger angiogenesis (Lozano

Submitted August 20, 2001, and accepted for publication January 9, 2002.

Moreno Zamai and Chithra Hariharan are equal contributors in this work.

Address reprint requests to Dr. Abraham H. Parola, Department of Chemistry, Ben Gurion University of The Negev, P.O. Box 563, Beer-Sheva, 84105, Israel. Tel: 972-8-6472454/6461188; Fax: 972-8-6472943; E-mail: aparola@bgumail.bgu.ac.il.

0006-3495/02/05/2652/13 $2.00

et al., 1998; Ogura et al., 1999). This provided a mechanistic explanation for the observed increase in the affinity between FGFs and tyrosine kinase receptors in the presence of heparin (Lozano et al., 1998; Ogura et al., 1999). Residues involved in receptor recognition appear to be clustered in two separate patches on the FGFs, namely, high affinity receptors (HARs) binding sites and low affinity receptors binding sites (Lozano et al., 1998).

It has been shown that the recognition of bFGF by HARs requires the bFGF to be previously bound to heparin. The binding to heparin induces conformational changes that extend well beyond its binding site and affects the whole structure of the protein. These changes cause a net decrease in the flexibility of the protein, which affects the regions on bFGF that interact with the HARs (Lozano et al., 1998).

Since the demonstration of the role of angiogenesis in cancer, the search for angiogenesis inhibitors has become the focus of several research groups (Herblin et al., 1994; Auerbach and Auerbach, 1994). In the last few years, naphthalene sulfonic distamycin-A derivatives were shown to inhibit the binding of human recombinant bFGF to its receptors, to block in vivo bFGF-induced vascularization and to stop neovascularization in chorioallantoic membrane (Ciomei et al., 1993). Suramin is one such polysulfonated naphthylurea that was examined as a potential anticancer drug (La Rocca et al., 1990; Kohler et al., 1992; Braddock et al., 1994; Manetti et al., 1998, 2000). Inhibition of FGF activity in the presence of suramin has been attributed to the formation of nonspecific and irreversible protein aggregation. However, an important limitation on the clinical use of suramin is the narrow margin between the dose required for antitumor activity and that leading to the onset of prohibitive toxic side effects (Middaugh et al., 1992). Therefore, any drug with similar antitumor activity as suramin but substantial lower toxicity would be of considerable potential value. In this regard, a distamycin A derivative, (7,7-(carbonyl-bis[imino-*N*-methyl-4,2-pyrrolecarbonylimino[*N*-methyl-4,2-pyrrole]-carbonylimino])-bis-(1,3-naphthalene disulfonate)) - PNU145156E (suradista) was shown to inhibit the growth of murine tumors with relatively low toxicity (Sola et al., 1995, 1999). Unlike suramin, PNU145156E does not cause caotropic aggregation of proteins. Our results on the interaction between this drug and bFGF revealed a 1:1 tight but reversible complex (Zamai et al., 1997, 1998). It is most likely that this interaction covers a large surface of the protein involving the heparin-binding domain described by Thompson et al. (1994) and the selenate-binding site proposed by Eriksson et al. (1993). Biologically effective dimerization of bFGF is mediated through heparin binding. The binding of PNU145156E to bFGF prevents this dimerization. Structural information on the interaction of suradista and suramin with FGFs is unavailable at present (attempts to crystallize the complex failed). Gallego and co-workers have attempted structural analysis using heparin and suramin functional analogs (MIHS and naphthalene trisulfonate (NTS), respectively) (Pineda-Lucene et al., 1998). They found that NTS and MIHS binding sites partially overlap.

The intrinsic tryptophan fluorescence of the protein and the weak drug fluorescence may be used to characterize the protein-drug binding interactions. As opposed to other spectroscopic techniques that require much higher concentrations of the interacting molecules, which eventually cause aggregation, fluorescence detection requires micromolar concentrations of the interacting molecules. Fluorescence quenching of the protein (Trp) by PNU145156E and the energy transfer band of PNU145156E were monitored to quantify the binding interaction and to obtain the distance information between the protein and the drug. Fluorescence lifetime and anisotropy were used to compute the binding constant and also the stoichiometry of the complex. In addition, site-directed mutagenesis at the heparin-binding site involving the residues identified by Eriksson et al. (1993) (e.g., K128, K134, K138, and a double mutant of K128-K138) should markedly affect the binding of the drug. The change from each lysine (K) to glutamine (Q) upon mutation reduces a single positive charge required to neutralize the sulfates in the drug. The consequent loss of electrostatic interaction should decrease the binding of the drug on the putative docking site and affect both the thermal stability and compactness of the protein. Temperature profiles of the binding curves were used to explore the kinetics and thermodynamic stability of this complex. Finally, a model of the protein-drug binding is proposed.

MATERIALS AND METHODS

Reagents and solutions

Suradista (PNU145156E), tetra sodium salt (molecular weight 1273, 98% purity assessed by elemental analysis and nuclear magnetic resonance) was obtained from Pharmacia and Upjohn (Milan, Italy). Human recombinant fibroblast growth factor (bFGF) was purchased from PeproTech (Rocky Hill, NJ). Its mutants K128Q, K138Q, K134Q, and K128Q-K138Q and the heparin functional analog, β-cyclodextrin tetradecasulfate (β-CDS), were prepared at A.Y.'s laboratory (Yayon et al., 1991; Li et al., 1994). Phosphate-buffered saline (PBS) contains 7.5 mM NaH_2PO_4, 17.5 mM Na_2HPO_4, and 0.15 M NaCl (pH 7.1). A constant temperature bath (RTE-111, Neslab Instruments, Inc., Newington, NH) with accuracy ± 0.1°C was used for temperature studies.

Fluorescence measurements

Steady-state fluorescence anisotropy and lifetime measurements were performed on a fully automated frequency domain spectrofluorometer (ISS-K2, ISS, Urbana-Champagne, IL) equipped with a 300-W Xenon arc lamp, Glan polarizers, and a constant temperature bath. Samples were placed in a 1-mm path cuvette (approximate volume of 100 μL, Hellma, Jena, Germany). For reference, we used TiO_2 scattering solution. The emission of tryptophan was collected using a Kodak UG1 filter that transmits light above 320 nm. The noise levels were typically 0.3 to 0.5° in phase angle and 0.005 to 0.010 in modulation. Data were analyzed by the ISS-K2 software. Fluorescence titration was performed for wild-type bFGF and its mutants with increasing concentrations of PNU145156E in PBS. Total sample absorptivity was lower or equal to 0.2 optical density. For anisot-

ropy titration, the G factor was determined for correction. Quinine sulfate (1 μM in 0.1 N sulfuric acid) was used as the quantum counter. Steady-state fluorescence and lifetime measurements were done at 25°C. Temperature profiles of the binding were taken between 7°C and 35°C. Dynamic polarization measurements for the bFGF:PNU145156E complex were performed using the single photon counting setup at Prof. Elisha Haas' Laboratory at Bar Ilan University (Gottfried and Haas, 1992; Haas, 1996): (tryptophan, λ_{ex} = 295 nm, λ_{em} = 340 nm; PNU145156E, λ_{ex} = 350 nm, λ_{ex} = 450 nm; energy transfer λ_{ex} = 295 nm, λ_{em} = 450 nm).

Determination of dissociation constants

Fluorescence steady state and lifetime titrations were used to determine the dissociation constant (K_d) of bFGF:PNU145156E complex. bFGF concentration was kept constant (0.31 μM in PBS) with increasing PNU145156E concentrations. The experiments were performed under equilibrium conditions (Zamai et al., 1998). The model of simple bimolecular association with ligand depletion was used to calculate binding constant (Hulme and Birdsall, 1992). The binding curves at different temperatures were constructed for the wild type and two of the mutants (K128Q and K128Q-K138Q). Values of K_d (or K_a) were determined using the Prism program, from GraphPad Software Inc. (San Diego, CA).

Determination of R_0

Förster distance, R_0, is the distance between the donor and the acceptor for a 50% efficiency of resonance energy transfer (Förster, 1965). This constant is calculated using the spectroscopic properties of the donor and the acceptor: a refractive index (n_D) of 1.337 was used for PBS. The fluorescence quantum yield of the donor molecules was determined with reference to quinine sulfate solution (in 0.1 N H_2SO_4) with a quantum yield of 0.55. The spectral overlap integral J (M^{-1} cm^{-1} nm^4) between the emission spectrum of tryptophan residue in the protein and the absorption spectrum of PNU145156E is given by:

$$J = [\sum F_D(\lambda) A_A(\lambda) \lambda^4 \Delta\lambda] / [F_D(\lambda) \Delta\lambda] \quad (1)$$

The orientation factor (κ^2) depends on the relative orientation of the transition dipoles of the donor and the acceptor. The first estimation of the Förster distance is obtained by fixing the isotropic dynamic average value of $\kappa^2 = 2/3$ into the equation.

The ratio of steady-state fluorescence intensities for the donor only (I_D) and the donor in the presence of acceptor (I_{DA}) is proportional to the average energy-transfer efficiency $\langle E \rangle$ (equals 1, for 100% efficiency), as described below:

$$\langle E \rangle = 1 - I_{DA}/I_D \quad (2)$$

The measured energy-transfer efficiency was used to calculate the average distance $\langle R \rangle$ between the donor and the acceptor transition dipoles (see legend of Table 3).

Estimation of the range of κ^2

From the measured emission anisotropy one can estimate the range of κ^2 using Eqs. 3 and 4 given by Blumberg et al. (1974) and Dale et al. (1979):

$$\langle \kappa^2 \rangle_{max} = 2/3(1 + \langle d_{D^x} \rangle + \langle d_{A^x} \rangle + 3\langle d_{D^x} \rangle \langle d_{A^x} \rangle) \quad (3)$$

$$\langle \kappa^2 \rangle_{min} = 2/3[1 - (\langle d_{D^x} \rangle + \langle d_{A^x} \rangle)/2] \quad (4)$$

in which

$$\langle d_{D,A^x} \rangle = (r_p/r_0)_{D,A^{1/2}}, \quad (5)$$

$\langle d_{D,A^x} \rangle$ is the donor or acceptor depolarization factor, r_p is the experimentally determined limiting anisotropy of either the attached donor or the attached acceptor each excited at its absorption band, and r_0 is the observed fundamental anisotropy of either the free donor or the free acceptor. The limiting anisotropy is independent of the rotational motion of the macromolecule and reflects the orientation of the attached chromophores. For PNU145156E, $\langle d_{A^x} \rangle = 1$ (for a rigid binding). For the donor (tryptophan in bFGF) $\langle d_{D^x} \rangle \sim (0.05/0.3)^{1/2} = 0.41$, using anisotropy values r_p experimentally obtained by us and r_0 by Hansen et al. (1992).

Temperature dependence of binding kinetics

The change in the fluorescence intensity of tryptophan emission after the addition of PNU145156E was monitored as a function of time at different temperatures. A difference signal was collected after subtracting the fluorescence of the sample from control.

Circular dichroism

Circular dichroism (CD) spectra of PNU145156E and bFGF, at different concentrations, were recorded against the respective blanks by a J-715 spectropolarimeter (Jasco, Hanover, Germany), equipped with a 150-W Xenon arc lamp, double polarized prisms monochromator Czerny-Turner (from Acton Research, Acton, MA), and piezoelectric modulator. For calibration, nonhygroscopic, water-soluble ammonium *d*-10-camphorsulfonate was used. Cuvettes of 1-mm optical pathway were used. Spectra of bFGF (0.9–1.4 μM) in PBS at variable pH in 290 μL final volume were recorded in the range of 195 to 260 nm. The titration to different pH was obtained using 100 mM 3-([3-cholamidopropyl]-dimethylammonio)-1-propanesulfonate for pH ranging between 7.7 and 9.8.

Thermal denaturation of bFGF

Thermal denaturation of bFGF was followed at 278 nm, applying a gradient of 1°C/min from 27°C to 78°C and from 40°C to 90°C. The enhanced ultraviolet absorption was monitored with a Perkin-Elmer (BSW, Bodensewerk, Uberlingen, Germany) Lambda 11 spectrophotometer, equipped with a temperature-controlled cuvette holder and an LKB 2219 Multitemp II Thermostatic Circulator (±0.1°C), from Amersham Pharmacia Biotech (Uppsala, Sweden).

RESULTS AND DISCUSSION

Several amino acid residues in bFGF, Lys^{35}, Asn^{36}, Arg^{90}, Lys^{128}, Arg^{129}, Gln^{132}, Lys^{134}, Lys^{138}, Gln^{143}, and Lys^{144} (based on the sequence given in Eriksson et al. (1991, 1993) and Thompson et al. (1994) and the numbering system given by Li et al. (1994)) form the discontinuous epitope of the binding site for heparin (Fig. 1). Residues 115 to 124, presumed to bind to the receptor, include an irregular loop that extends from the surface of bFGF and is ~25 Å away from the heparin-binding site. It is known that the above lysine side chains form salt bridges with sulfate moieties in heparin (Li et al., 1994). In a previous publication (Zamai et al., 1998) we suggested that PNU145156E covers a large surface of the protein that includes the heparin-binding

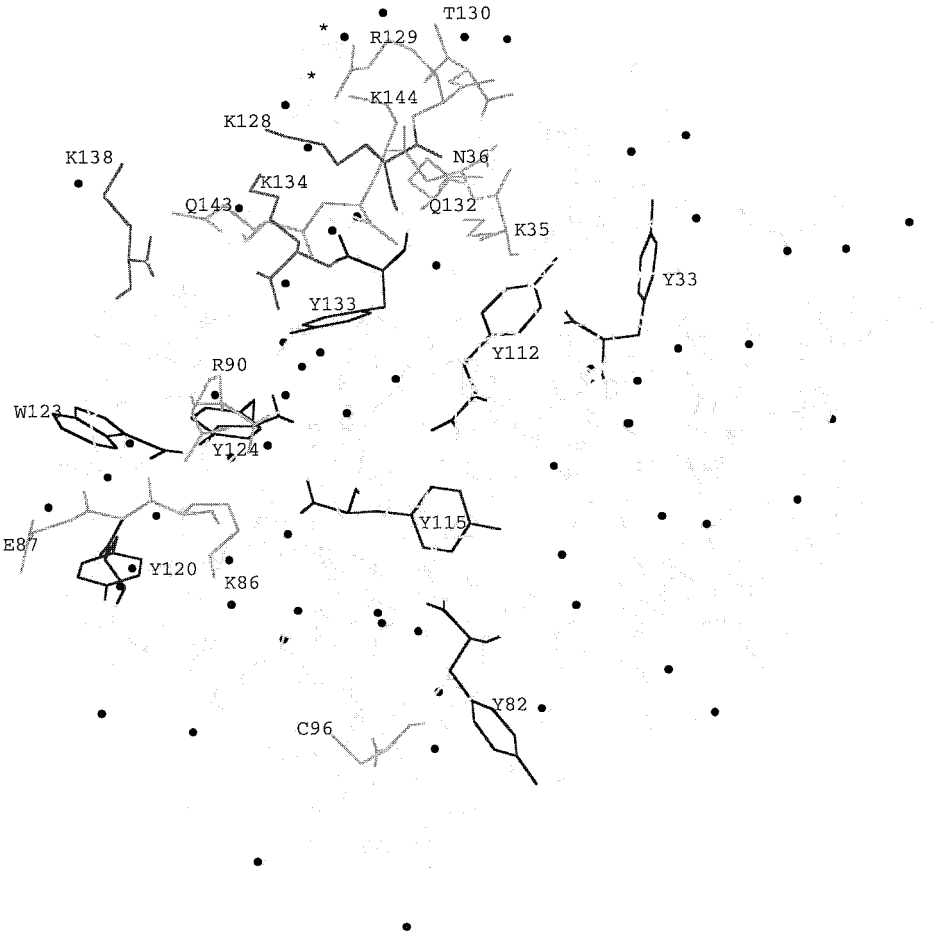

FIGURE 1 X-ray structure of human bFGF, taken from the PDB (Eriksson et al., 1993). Structure was obtained at 1.6-Å resolution. The protein was expressed in yeast (*Saccharomyces cervisiae*). Asterisks (*top*) denote sulfate groups at the presumed heparin-binding site. The relevant amino acids mentioned in the manuscript are marked, including the seven tyrosines and tryptophan-123. Dark dots reflect water molecules. The measured diameter of the protein ranges from 34 to 40 Å.

domain described by Thompson et al. (1994) and the selenate binding site proposed by Eriksson et al. (1993).

Steady-state fluorescence anisotropy measurements of the binding between bFGF and PNU145156E resulted in a saturation curve (Zamai et al., 1998; Fig. 2 *A*). To identify the binding site of PNU145156E on bFGF, the heparin-6 (molecular weight = 6000) was used in a competition study (Fig. 2 *B*). Free PNU145156E in buffer solution, at the concentration used for the binding studies, showed an anisotropy value of $r = 0.023 \pm 0.009$. This value was not altered in the presence of an equimolar concentration of heparin-6. The addition of heparin to the bFGF: PNU145156E complex resulted in a progressive decrease of PNU145156E fluorescence anisotropy from 0.126 ± 0.006 to that of the free ligand, 0.030 ± 0.010 (Fig. 2), suggesting that heparin displaces the drug from the complex, and further supports the reversibility of the interaction. Moreover, 50% displacement occurs when the concentrations of heparin and PNU145156E were approximately the same, leading to relative K_d values of 142 ± 16 and 54 ± 6 nM (mean $\pm$ SD, $n = 8$) for PNU145156E and heparin, respectively. These results are expected in view of the similar dissociation constants reported by Thompson et al. (1994) for heparin, and by us for PNU145156E (Zamai et al., 1998), obtained under similar ionic strength (Table 1). These observations imply that both PNU145156E and heparin compete for the same binding area, sharing at least one binding site.

The good overlap between tyrosine (Fig. 3 *A*) or tryptophan (Fig. 3 *B*) emission spectrum and PNU145156E excitation spectrum (Fig. 3 *C*) renders both donor-acceptor pairs suitable for efficient Förster energy transfer. The 80% fluorescence quenching of the seven tyrosine residues in bFGF by PNU145156E (shown in Fig. 4) resulted in a linear Stern-Volmer plot (Fig. 4 inset). Because tyrosines 33, 112, 115, 120, 124, and 133 are located ~15, 16, 17, 11, 13, and ~10 Å, respectively, from the sulfonates binding site, and tyrosines 82 and 115, ~12 and 20 Å from the selenate binding site (Fig. 1), they were expected to be efficiently quenched. Therefore, whereas inner filter effects caused by PNU145156E could contribute to the observed quenching, energy transfer must play a major role. The quenching of the single Trp^{123} was associated with an increase in the fluorescence emission of PNU145156E at 440 nm, resulting from energy transfer, Fig. 5. Because Trp^{123} is located ~16 and 15 to 20 Å from the heparin and the selenate putative

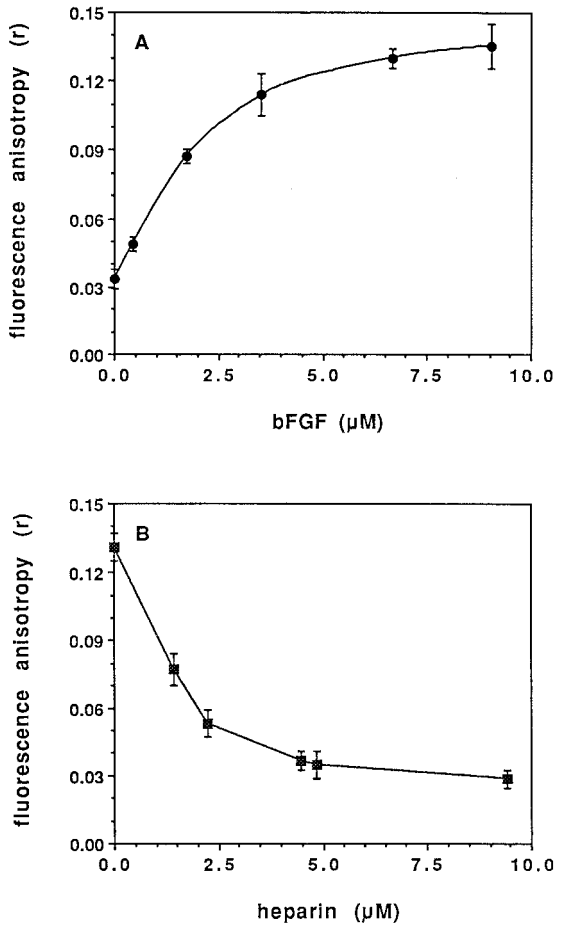

FIGURE 2 Binding of PNU145156E to bFGF (*A*) and displacement of PNU145156E from PNU145156E:bFGF complex by heparin-6 (*B*). Steady-state fluorescence anisotropy was measured at λ_{ex} = 350 and λ_{em} = 440 nm in PBS, pH 7.1, at 20°C. [PNU145156E] = 1.94 μM; [bFGF] = 2.9 μM.

binding sites in bFGF, respectively (Fig. 1), the observed energy transfer further support the hypothesis of a common binding cleft for heparin and PNU145156E.

Three single mutants (K128Q, K134Q, and K138Q) and a double mutant (K128Q-K138Q) in the heparin-binding cleft were studied. Steady-state tryptophan fluorescence quenching of wild-type bFGF and its mutants by PNU145156E and by the heparin functional analog β-CDS, as well as steady-state and time-resolved fluorescence measurements of PNU145156E, led to the binding constants shown in Table 2. The magnitude of the K_d values revealed that the same basic lysine residues that were identified to be on the heparin-binding domain are also essential for binding with PNU145156E. The replacement of each lysine residue (K) in the single and the double mutants by neutral glutamine (Q) resulted in an average of ~5- to 10- and 30- to 40-fold decrease in the binding constants, respectively (Table 2). This would translate to a ΔG_0 loss of ~6 to 10 kJ mol^{-1} (Table 2). The similar change of ΔG_0 values, regardless of the site at which the positive charge is eliminated, indicates that the binding is stabilized by the charge density in the binding cleft, each charge contributes roughly 5 kJ mol^{-1} to the total binding interaction. That is, the electrostatic energy is about linear with the charge density on the interacting surface.

TABLE 1 Comparison of dissociation constants associated with the binding of PNU145156E and heparin to wild-type bFGF and its mutants

bFGF	PNU145156E* (150 mM)	Heparin† (150 mM)	Heparin‡ (10 mM)	Heparin‡ (150 mM)
	K_d (nM)			
Wild type	127 (1)§	470 (1)	2.3	214 (1)
K128Q	1230 (9.7)	—	19.3	1796 (8.4)
K128A	—	1670 (3.6)	—	
K134Q	1147 (9.0)	—	0.4¶	37 (0.2)
K134A	—	7890 (16.8)	—	
K138Q	1157 (9.11)	—	10.8	1008 (4.7)
K138A	—	1460 (3.1)	—	
K128Q-K138Q	5115 (40.3)	—	247.7	23,074 (107.9)

*The *average* values taken from Table 2.
†Taken from Thompson et al., 1994.
‡Taken from Li et al., 1994.
§Shown in parenthesis are factorized values in which the dissociation constant obtained for the wild type, in each column, is presented as 1.
¶Additional studies have shown that the K_d value for K134Q reported by Li et al. (1994) is questionable.

Table 1 summarizes the K_d values for wild-type bFGF and its mutants obtained by Thompson et al. (1994) and Li et al. (1994) with heparin, and by us, with PNU145156E. Whereas Thompson et al. (1994) and we used buffers with similar ionic strength (150 mM) Li et al. (1994) results were obtained at lower ionic strength (10 mM). For the sake of comparison, Li et al. data were factorized for the ionic strength of 150 mM, using the calibration curve shown in Fig. 5 in Thompson et al. (1994). A direct comparison between our and Thompson et al. (1994) results is justified because both types of mutations used (alanine and glutamine, respectively) resulted in the diminution of a single positive charge per amino acid replaced at the binding cleft of heparin. Inspection of the values obtained after correction for the ionic strength reveals similar K_d values for heparin (Li et al., 1994; Thompson et al., 1994), within the same order of magnitude as our K_d values for PNU145156E. Thompson et al. (1994) have found ~37% contribution of electrostatic interaction to the total binding interaction. Comparison with our results, based on the linear correlation obtained between the lifetime values of PNU145156E and either Krygowski and Fawcett or Taft's multiparameter treatment of solvent polarity, revealed at least a similar contribution from polar interactions (Zamai et al., 1998). Additional support for the contribution of electrostatic interactions is obtained from the effect of double mutation, which, in free energy scale, is roughly additive. Thus, the

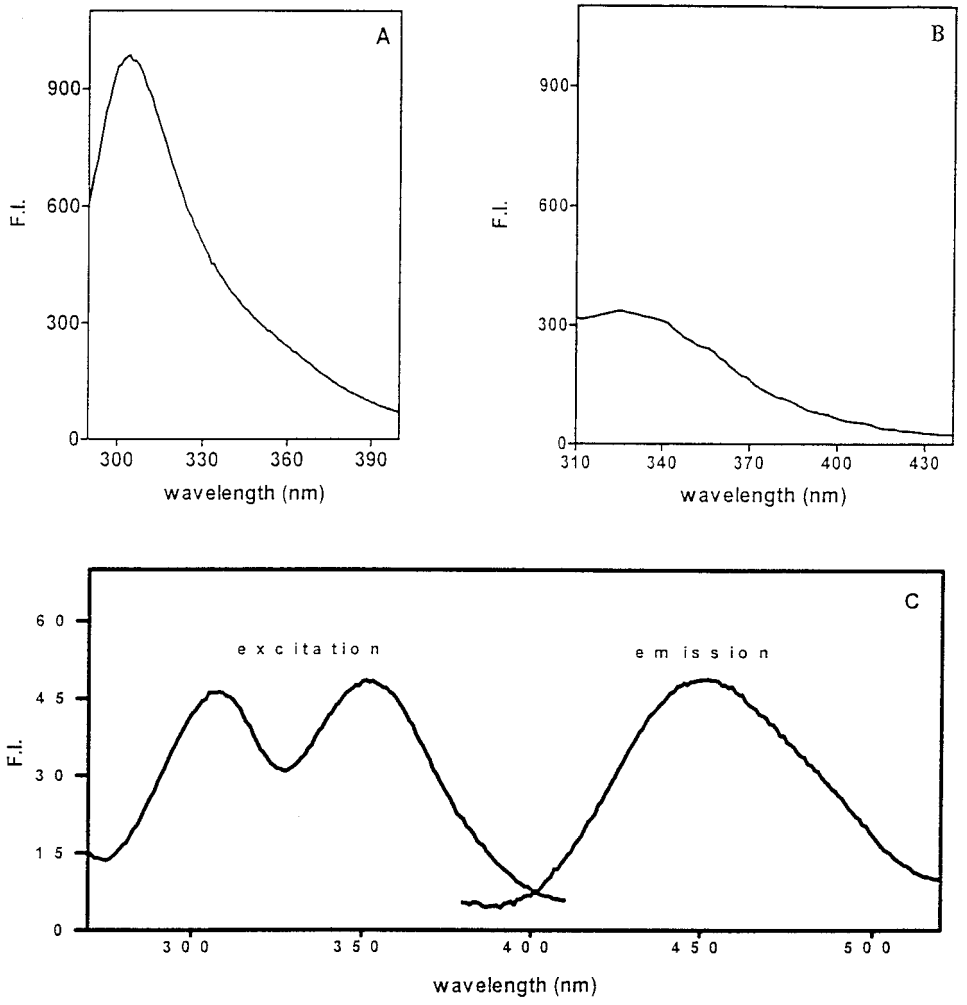

FIGURE 3 Corrected fluorescence spectra for the emission of bFGF and for the excitation and the emission of PNU145156E. The spectra were obtained in PBS, pH 7.1, at 22°C. bFGF (1.4 μM), was excited at 274 nm (*A*) and at 293 nm (*B*) for tyrosine and tryptophan emission, respectively. (*C*) PNU145156E (1.9 μM); the two excitation bands detected at 307 and 351 nm contributed equally to the emission.

electrostatic energy is about linear with the charge density on the surface of binding.

Förster type energy transfer analysis was carried out with the tryptophan-PNU145156E pair, in which the single tryptophan at position 123 of bFGF acts as the donor and PNU145156E acts as the acceptor. Fig. 6 shows the quenching curves obtained for wild-type bFGF and its mutant. The efficiency parameter of energy transfer $\langle E \rangle$, was obtained by extrapolating the quenching curves to binding saturation, as described in Materials and Methods. Table 3 summarizes these *E* values for the wild-type bFGF and its mutants. The observed decline in *E* values upon single and double mutations inversely correlates with the dissociation constants, i.e., the lower the dissociation constant the higher is the efficiency. This shows that the complex becomes weaker as the number of positive charges and the corresponding coulombic attractions are reduced. Attempts to calculate the corresponding distances between PNU145156E and wild-type bFGF and its mutants were based on the calculated Förster distance R_0 = 14.03 Å, using κ^2 = 2/3, because from the crystal structure of bFGF, the tryptophan chro-

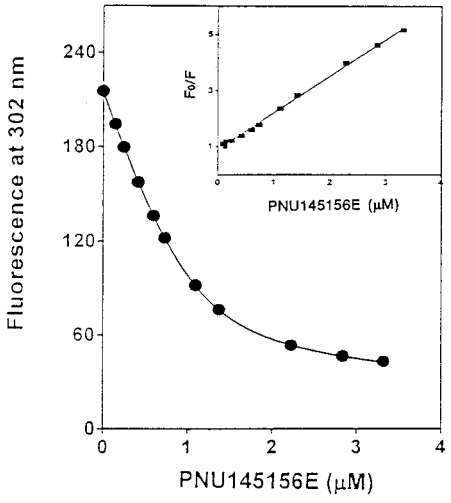

FIGURE 4 Quenching of bFGF-tyrosine fluorescence emission by PNU145156E in PBS, pH 7.1, at 22°C. λ_{ex} = 274 nm; λ_{em} = 302 nm; [bFGF] = 1.15 μM. The best nonlinear least-square fit, based on Hulme and Birdsall (1992), is presented by the solid line. (*Inset*) Stern-Volmer analysis based on: the solid line is the fitting to $F_0/F = 1 + K_{sv}$ [PNU145156E], in which K_{sv} is the Stern-Volmer quenching constant.

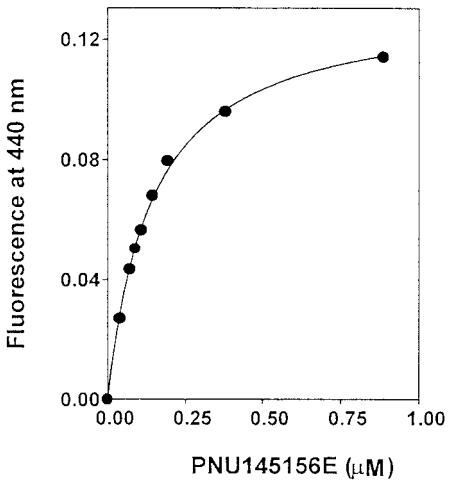

FIGURE 5 Energy transfer in bFGF:PNU145156E complex. The increase in PNU145156E fluorescence emission intensity at λ_{em} = 440 nm, upon excitation at λ_{ex} = 293 nm (bFGF-tryptophan), was followed using 0.34 μM bFGF in PBS, pH 7.1, at 22°C, as a function of [PNU145156E]. Energy transfer data analysis was carried out applying the one site binding mode (hyperbola): $A = (A_\infty[D])/K_d + [D])$ in which A is the fluorescence intensity, A_∞ is the maximal fluorescence intensity, and [D] is the molar concentration of PNU145156E.

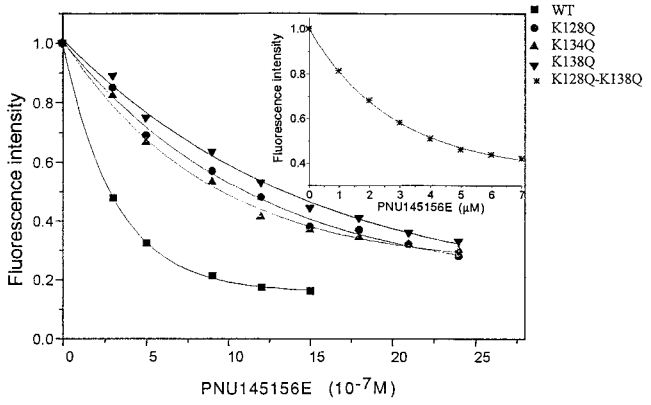

FIGURE 6 Fluorescence quenching of wild-type bFGF and its mutants by PNU145156E. The fluorescence emission of Trp^{123} of bFGF, wild-type, and its mutants, each at 0.31 μM, in the presence of variable concentrations of the suradista, PNU145156E, in PBS, pH 7.1, was followed at 25°C, λ_{ex} = 295 nm, λ_{em} = 340 nm. The efficiency of energy transfer was obtained by extrapolating the quenching curves to binding saturation, as described in Materials and Methods. (*Inset*) The fluorescence emission of the double mutant K128Q-K138Q. Note the units of concentration in the abscissa.

mophoric side chain is aqueously exposed and free to rotate on the surface of the protein (Fig. 1). Regardless of its free rotation, because of the rigid binding of PNU145156E, the values of κ^2 could span from 0.2 to 2.4, which translate into a range from $R_0((\kappa^2_{max})^{1/6})$ to $R_0((\kappa^2_{min})^{1/6})$ = (1.0 ± 0.2)R_0, using Eqs. 3 and 4 (in Materials and Methods). Table 3 presents the calculated R values. After mutation R value increased by ~20% in the single mutants and by ~30% in the double mutant. Because the changes are small, the tightness of binding is thus reflected: with more positive charges and corresponding attractive coulombic interactions, the distance between PNU145156E and tryptophan at the binding cleft became shorter. Table 4 reports on the rotational correlation times observed for free wild-type bFGF and its mutants. These were practically identical and averaged at 6.1 ± 0.1 ns (mean ± SD, n = 4) and resulted in similar radii values. Thus, it is suggested that no significant conformational changes occurred upon point mutation in free bFGF. The displaced volume of the complexes, 24,200 ± 400 Å^3, was calculated from the rotational correlation time, assuming a rotating sphere (Courtney and Fleming, 1985). This was based on Stokes'-Einstein equation, $\phi = V_\eta/k_BT$ in which k_B is Boltzmann constant, T is the absolute temperature, V is the displaced volume of the rotor, and η is the viscosity (~1.02 cP). Because the average radius of wild-type bFGF and its mutants is 18.0 ± 0.2 Å, it may be concluded that the overall dimensions of the protein remains unaltered during mutation. This does not exclude local conformational changes in the binding cleft.

TABLE 2 Binding constants and associated free energies for the formation of bFGF:PNU145156E and bFGF:β-CDS complexes

	bFGF:PNU145156E						bFGF:β-CDS		
	K_d* (nM)				$\Delta G^\ddagger$	$\Delta\Delta G^\S$	$K_d^\dagger$ (nM)	ΔG	$\Delta\Delta G^\S$
bFGF	Q	ET	τ	Average	(kJ mol^{-1})		Q	(kJ mol^{-1})	
Wild type	120	119	143	127	−39.42	—	118	−39.52	—
K128Q	1080	1061	1551	1230	−33.63	5.79	516	−35.87	3.65
K134Q	1000	983	1459	1147	−33.88	5.54	533	−35.79	3.73
K138Q	972	832	1667	1157	−33.73	5.69	546	−35.73	3.79
K128-138Q	4924	5306	5286	5115	−30.18	9.24	3207	−31.34	8.18

Wild-type bFGF and its mutants, each at 0.31 μM, were incubated in PBS with 0.01 to 2.5 μM PNU145156E or 0.01 to 1.0 μM β-CDS at 25°C. Dissociation constants were obtained by: Q, quenching of the Trp^{123}-bFGF fluorescence emission at 340 nm, either by PNU145156E* or β-CDS†, λ_{ex} = 295 nm; ET, energy transfer to PNU145156E measuring fluorescence emission at 450 nm, λ_{ex} = 295 nm, and τ, lifetime of PNU145156E.

$^\ddagger\Delta G_0 = -RT \ln [K_{d(Mutant)}/K_{d(wt)}]$.

$^\S\Delta\Delta G_0$ is the difference between the average ΔG_0 values of mutants and wild-type bFGF.

TABLE 3 Energy transfer efficiency parameters (*E*) and associated distances (*R*) obtained from steady-state fluorescence studies for bFGF-bound PNU145156E

bFGF	$\langle E\rangle$*	$R^{\dagger}$ (Å)
Wild type	0.84	10.6
K128Q	0.62	12.9
K134Q	0.70	12.2
K138Q	0.67	12.5
K128Q-K138Q	0.58	13.3

*$\langle E\rangle = [1 - (I_{DA}/I_D)]$.
†$R = R_0[(1 - \langle E\rangle)/\langle E\rangle]^{1/6}$; $R_0{}^6 = (8.79 \times 10^{-25})(n_{D^{-4}}\phi_D\kappa^2 J_{AD})$; $J = 3.2 \pm 10^{-16}$ cm^6 M^{-1}; $n_D = 1.337$ for PBS; $\phi_D = 0.13$; $\kappa^2 = 2/3$; $R_0 = 14.03$ Å.

The present study enabled us to compare the radius of wild-type bFGF obtained by tryptophan fluorescence anisotropy with that of its complex, which was obtained by PNU145156E fluorescence (Zamai et al., 1998). The increase of 0.7 Å in the average radius of the complex (Table 4) may suggest that PNU145156E fits well into the binding cleft, resulting in the proposed compact 1:1 complex (Zamai et al., 1998). The values shown in Table 4 seem to demonstrate that binding of PNU146156E to wild-type bFGF and its mutants did not cause a major change in the overall globular structure of the protein. Still, despite the uncertainty in choosing the model of a rotating sphere as well as the lack of significant differences between the radii values of free and bound proteins, opposing trends between the wild-type bFGF and its doubly mutated form upon complexation may take place. In the temperature studies and the corresponding thermodynamic analysis presented below, these trends became conspicuous. The volume of the complex with wild-type bFGF seems to expand relative to the free protein while that of the doubly mutated one decreases, suggesting differences in local conformational changes. It should also be pointed out that the calculated hydrodynamic volumes that revealed similar diameter values of ~36 Å, are similar to that measured from the x-ray structure of the protein (Eriksson et al., 1993), 34 to 40 Å (Fig. 1). The data presented in Tables 3 and 4 fit well with the x-ray crystal structure of bFGF (Fig. 1). One may notice that energy transfer may occur between Trp[123] and the naphthalenic chromophores of PNU145156E, which are the two coulumbic hooks: one which is anchored to the selenate binding site and the other is anchored to the heparin binding site, located ~11 to 12 and ~10 to 15 Å away, respectively. Based on these findings, together with the results obtained upon the carboxymethylation of bFGF (Zamai et al., 1998), the competition with heparin (Fig. 2) and the increase in K_d values upon mutation, the unique binding mode of the drug to both the heparin and the selenate binding sites gains much support.

TABLE 4. Effect of PNU145156E binding to bFGF on the radius (*r*) of the complex based on rotational correlation time (ϕ) measurements

bFGF	ϕ* (ns)	$r^{\dagger}$ (Å)	$\Delta r^{\ddagger}$ (Å)
Wild type	6.0	17.8	
Wild type + PNU145156E	6.7[§]	18.5[¶]	0.7
K128Q	6.2	18.2	
K128Q+PNU145156E	6.3	18.3	0.1
K138Q	6.2	18.2	
K138Q + PNU145156E	6.4	18.3	0.1
K128Q-K138Q	6.1	17.9	
K128Q-K138Q + PNU145156E	5.6	17.4	−0.5

*Rotational correlation times are the average of time resolved single photon anisotropy decay measurements for either bFGF alone (0.31 μM) or (where indicated) bFGF-bound PNU145156E (1.94 μM), using $\lambda_{ex} = 295$ and 340 nm, and $\lambda_{em} = 350$ and 450 nm, for tryptophan and PNU145156E, respectively, assessed at room temperature.
†Radii values obtained from the Stokes' Einstein equation, $\phi = V_\eta/k_BT$, assuming a rotating rigid sphere, see text.
‡Difference between the average radii values of bound and free bFGF.
§Average includes the value published before, 6.56 ns (Zamai et al., 1998).
¶Based on the average shown in §.

To gain an insight into the conformational changes occurring in bFGF upon binding to PNU145156E, CD measurements were performed. bFGF has a CD spectrum with a minimum at 205 nm. A strong effect on the 205-nm band was observed upon the addition of PNU145156E at 22°C (in PBS, pH 7.1; Fig. 7 *A*). The CD spectra as a function of pH also showed decrease in molar ellipticity (not shown). The effect caused by PNU145156E binding to bFGF resembled that observed for the free protein at pH 9.5 (Fig. 7 *B*).

Ultraviolet hyperchromism at 278 nm as a function of increasing temperature was used for studying the thermal stability of the protein. Fig. 8 depicts the thermal denaturation of wild-type bFGF in the presence of increasing concentrations of PNU145156E. A concentration-dependent increase in the plateau was observed with ~10°C shift of the midpoint of the curves toward lower temperatures, i.e., from a "melting temperature" T_m = 62.2 to 53.1°C. A simple two-state (folded-unfolded) model could not explain the concurrent increase of the absorbance plateau. Therefore, T_m values were calculated applying the Boltzmann's equation (Cantor and Schimmel, 1980). Yet, a first order kinetics, with $t_{1/2}$ = 14.4 min, was revealed when isothermal kinetic measurements were followed at 37°C by differential absorbance spectroscopy at 278 nm. These may suggest that conformational changes were induced upon PNU145156E binding.

The effect of temperature on the binding of wild-type bFGF and two of its mutants, K128Q and K128Q-K138Q, with PNU145156E was studied. The values of the thermodynamic parameters are shown in Table 5. van't Hoff plots (ln K_a versus inverse temperature, in the range of 5–45°C) showed that upon increasing temperature the binding of PNU145156E to wild-type bFGF and its mutants decreased, resulting in distinctly different shapes (Fig. 9). For the wild-type bFGF:PNU145156E complex, a concaved shape

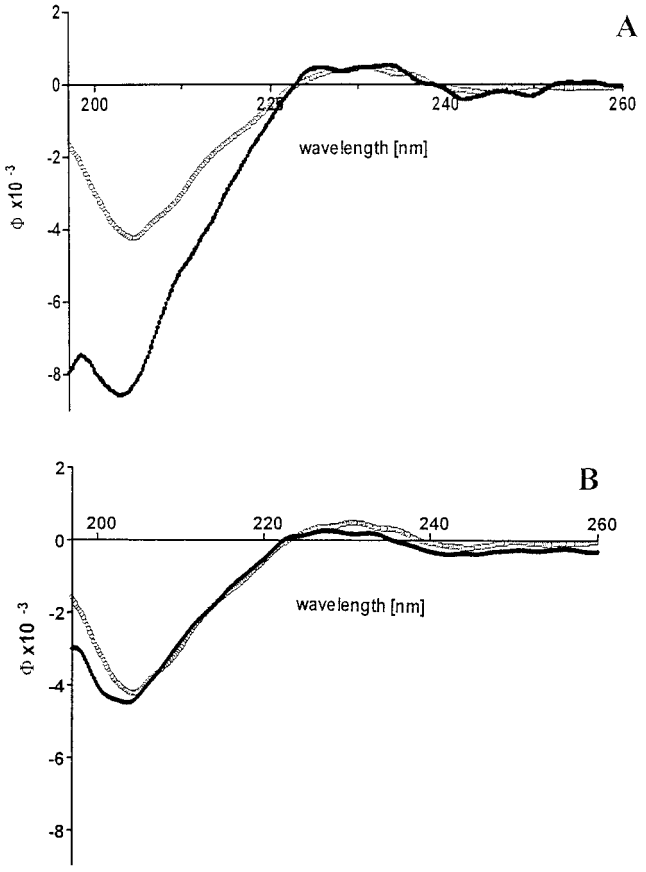

FIGURE 7 Effect of pH and binding to PNU145156E on the CD spectra of bFGF. Spectra of bFGF, free (●), and PNU145156E-bound (○) recorded in PBS, pH 7.1, at 22°C (*A*) and at pH 9.5 (*B*). Spectra of bFGF:PNU145156E complex, recorded in PBS, pH 7.1, at 22°C (*A* and *B*). [bFGF] = [PNU145156E] = 1.5 μM.

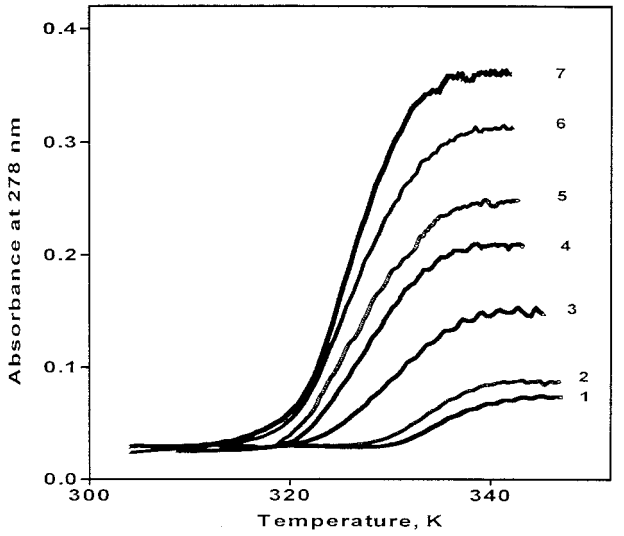

FIGURE 8 Effect of PNU145156E on the thermal stability of bFGF. To evaluate the thermal stability of bFGF, ultraviolet hyperchromism at 278 nm as a function of increasing temperature was obtained using 1.15 μM bFGF in the absence (*1*) and the presence of: 0.25 (*2*), 0.55 (*3*), 1.2 (*4*), 1.6 (*5*), 2 (*6*), and 2.6 (*7*) μM PNU145156E. Each sample was preincubated at room temperature for 1 h, then a thermal gradient of 1°C/min was applied. Data were corrected for blank curves run at each ligand concentration.

was revealed (Fig. 9 *a*); the single mutant K128Q-bFGF: PNU145156E complex showed a linear plot (Fig. 9 *b*), whereas the complex with the double mutant, K128Q-K138Q-bFGF-PNU145156E, resulted in a convex shape (Fig. 9 *c*).

The van't Hoff equation

$$d(\ln K)/dT = \Delta H/RT^2 \quad (6)$$

is usually integrated to give a linear dependence on inverse temperature. When ΔH is temperature independent

$$\ln K = \ln Y - \Delta H_{vH}/RT \quad (7)$$

in which K is the binding constant, Y is the intercept value related to entropy, ΔH_{vH} is the so-called van't Hoff enthalpy, R is the gas constant, and T is the absolute temperature. If the enthalpy is assumed to depend linearly on temperature, i.e., with a temperature-independent nonzero heat capacity change (ΔC_p), then

$$\Delta H_{vH} = \Delta H_r + (\Delta C_p)(T - T_r) \quad (8)$$

in which ΔH_r is the enthalpy at the reference temperature T_r (T_r has been chosen so that ΔH_r is zero), then the integrated van't Hoff equation yields

$$\ln K = \ln K_r + \Delta C_p[-(1 + \ln T_r) + T_r/T + \ln T]/R \quad (9)$$

The solid lines in Fig. 9, *a* and *c*, were obtained by fitting the data to Eq. 4 with the following parameters: $\ln K_r = 14.3$, $T_r = 326$ K and $\Delta C_p = 730$ cal mol^{-1} K^{-1} and $\ln K_r = 12.8$, $T_r = 287$ K and $\Delta C_p = -2170$ cal mol^{-1} K^{-1}, respectively. The solid line in Fig. 9 *b* was obtained from linear regression of the van't Hoff Eq. 2, assuming implicitly that the enthalpy is temperature independent ($\Delta C_p = 0$). These data produced ΔH_{vH} value of -3960 cal mol^{-1}. Based on the analysis given by Spolar and Record (1994), the net entropy change at the characteristic temperature where $\Delta S^o_{assoc} = 0$ is assumed to consist of three contributions:

$$\Delta S^o_{assoc} = \Delta S^o_{HE} + \Delta S^o_{rt} + \Delta S^o_{other} \quad (10)$$

in which ΔS^o_{assoc} is the entropy change upon protein ligand association, ΔS^o_{HE} is the contribution from the hydrophobic effect, ΔS^o_{rt} is the contribution from rotational and translational changes, and ΔS^o_{other} is mainly the contribution from conformational changes. The enthalpy intercept of the enthalpy-entropy compensation plot (ΔH vs. $T\Delta S$) gives the enthalpy when $\Delta S^o_{assoc} = 0$ (Fig. 10). This occurs at $T = 315$ and 293 K and resulted in slopes = 1.06 and 1.07, for the wild-type bFGF and its double mutant, respectively. The

TABLE 5 Thermodynamic parameters (ΔG, ΔC_p, ΔH, and ΔS) and changes in surface area (ΔA_{np}) associated with the formation of bFGF: PNU145156 complex

bFGF	ln K_r*[†]	T_r*	ΔG_r*	ΔC_p	ΔH_s[‡]	EECS[§]	ΔS_{HE}	ΔS°_{conf}	ΔA_{np}
Wild type	14.3	326	−9240	730	−8510	1.06 (315 K)	−200	250	3090
K128Q[¶]	13.7	NA	−8290	0	−3960[‖]	NA	0	65	0
K128Q-K138Q	12.8	287	−7260	−1110	−7210	1.07 (293 K)	410	−360	−4660

*Subscript r denotes that the respective value is given at the temperature (T(K)) in which $\Delta H_{vH} = 0$, and [†]K_r is the association constant (nM^{-1}); ΔG, cal mol^{-1}, ΔC_p, cal mol^{-1} K^{-1}, ΔH, cal mol^{-1}, ΔS, cal mol^{-1} K^{-1}, ΔA_{np}, $Å^2$. [‡]$\Delta H_S = \Delta H$ at $\Delta S = 0$. [§]EECS, enthalpy enthropy compensation slope. [¶]Data given for T = 304K. [‖]ΔH based on van't Hoff equation (Eq. 6).
NA, not applicable.

hydrophobic contribution as a function of temperature can be estimated from Spolar and Record (1994):

$$\Delta S_{HE} = 1.35 \Delta C_p \ln(T/386) \quad (11)$$

The value 1.35 is an empirical factor found for protein folding and may be assumed to reasonably apply for the association of globular proteins with ligands (Faergeman et al., 1996). For rigid body association, $\Delta S^\circ_{rt} \sim -50$ cal mol^{-1} K^{-1} (Table 3, in Spolar and Record, 1994). Finally, we assumed that $\Delta S^\circ_{other} = \Delta S^\circ_{conf}$, which is an acceptable assumption in protein ligand association processes. Accordingly, we found that ΔS°_{conf} equals 250 and −360 cal mol^{-1} K^{-1} for the wild-type bFGF and its double mutant, respectively. Furthermore, using the empiric relationship between ΔS°_{HE} and ΔA_{np} (Spolar and Record, 1994)

$$\Delta S^\circ_{HE} = 0.32 \Delta A_{np} \ln (T/386) \quad (12)$$

in which ΔS°_{HE} is the entropy change due to the hydrophobic effect and ΔA_{np} is the change in the nonpolar surface area of the protein exposed to water. This area can be estimated, as given in Table 5.

The single and double mutants of bFGF, characterized by the reduction of one and two positive charges are progressively less stable than the wild-type bFGF (Li et al., 1994; Thompson et al., 1994). Binding of PNU145156E to wild-type bFGF results in destablization of the complex, as is evident from both the CD spectra (Fig. 7) and the temperature stability profiles (Fig. 8). The negative value of ΔH_s for all three proteins implies an enthalpy driven reaction. Based on ΔC_p values obtained upon binding of PNU145156E to the wild-type bFGF (Table 5), it is suggested that partial defolding occurred. In contrast, the binding of PNU145156E to the double mutant resulted in a negative ΔC_p value, which may indicate folding into a more

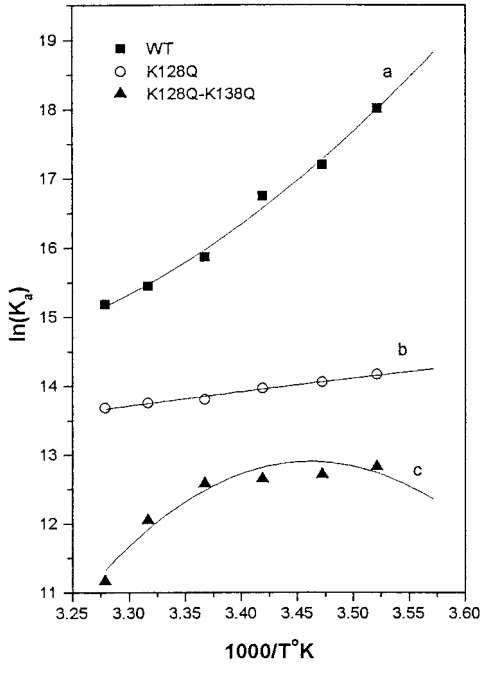

FIGURE 9 van't Hoff plots of the binding of wild-type bFGF and its mutants to PNU145156E. Straight line has been obtained assuming that $\Delta C_p = 0$. [protein], 0.31 μM; [PNU145156E], 1.94 μM.

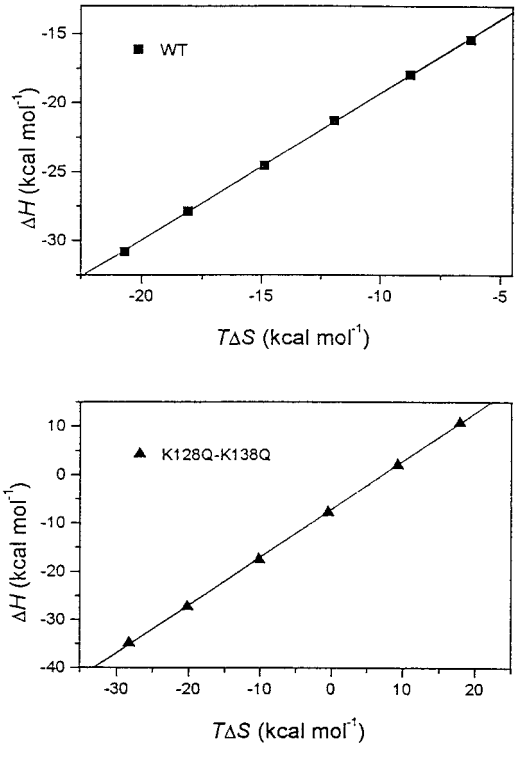

FIGURE 10 Enthalpy-entropy compensation plot. Data taken from Fig. 9 were used to obtain the ΔH versus $T\Delta S$ plots for the binding of wild-type bFGF and its K128Q-K138Q mutant to PNU145156E.

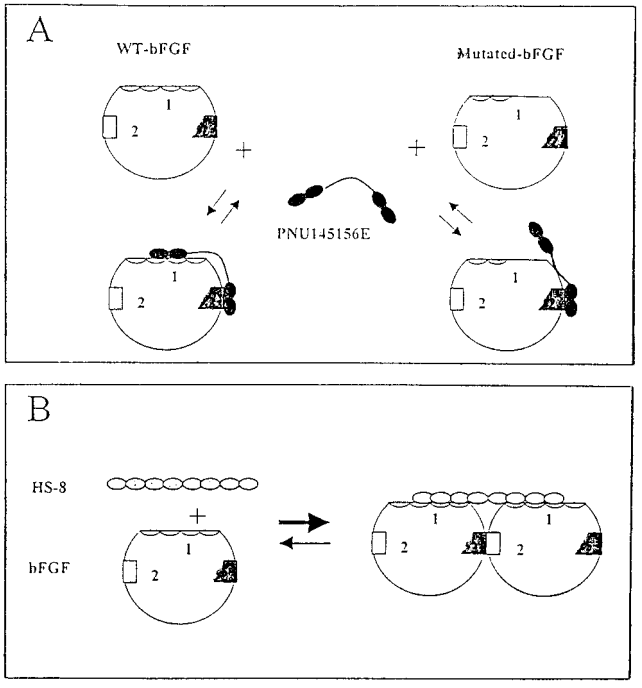

FIGURE 11 Proposed models for the interaction of PNU145156E and heparin, HS-8, with bFGF. (*A*) Complexation between PNU145156E and wild-type bFGF (*left*) and mutated bFGF (the substitution of the one-half circles by a straight line on top of the protein represents the reduction in positive charge) (*right*). (*B*) Herr's sketched model of *cis* bFGF:HS-8 dimer (Herr et al., 1997; Waksman and Herr, 1998).

compact conformation (Spolar and Record, 1994). This implies that the double mutant bFGF is more compact compared to the wild-type bFGF. This gains additional support from the change in entropy: the positive change in the entropy of conformation, ΔS^{o}_{conf}, upon complex formation with wild-type bFGF reflects the exposure of hydrophobic surface to water (meaning that water became less ordered due to breaking of the structured hydrogen bonding network in bulk water), and ΔA_{np} increased by 3090 Å^2 (Table 5). With the double mutant however, ΔS^{o}_{conf} value is negative and accompanied by a decrease of 4680 Å^2 in ΔA_{np}, which suggests the expulsion of protein-bound-water to the bulk (Table 5).

The data in Fig. 9 were then correlated with the experimentally determined distance between tryptophan and PNU145156E based on energy transfer data analysis given in Table 3: R = 10.6 and 13.3 Å for the wild-type and K128Q-K138Q bFGFs, respectively.

A proposed model of the interaction between bFGF and PNU145156E is presented in Fig. 11 *A*. Herr's sketched model of bFGF binding to the octasaccharide molecule of heparin, HS-8 (Herr et al., 1997; Waksman and Herr, 1998) is shown in Fig. 11 *B*. The *cis* bFGF-heparin complex is essential for bFGF binding to its receptor, a prerequisite for the activation of the angiogenic process (Herr et al., 1997; Waksman and Herr, 1998). In comparison, a proposed model for the interaction between bFGF and PNU145156E is shown in Fig. 11 *A*. PNU145156E binds to the cleft, which extends from the heparin binding site (1) to the selenate binding site, exploited by the protein for dimerization (2 or 2′) (Faham et al., 1996). Thus, the complexation with PNU145156E that blocks heparin binding and prevents protein dimerization can be a molecular level explanation for its antiangiogenic activity.

Based on x-ray crystallography, bFGF is assumed to be a sphere (Fig. 1). The bow-shaped PNU145156E with its charged naphthalenic ends and the hydrophobic polypyrrole skeleton in between may approach the wild-type protein in an extended conformation (Fig. 11 *A*, left). Thus, the positive charges on the bFGF (depicted schematically by the half circles on top of the protein) interact through coulombic forces as anchors for the negative naphthalenic edges of the bow shaped-PNU145156E serving as hooks. At least one water layer is left in between. In this mode of binding the distance between the donor Trp^{123} and PNU145156E acceptor chromophores was estimated from the energy transfer experiments to be 10.6 Å (Table 3). With the double mutant, PNU145156E approaches the protein sphere with one of its negative naphthalenic moieties away from the less positively charged heparin-binding edge (Fig. 11 *A*, right). This negatively charged naphthalenic end is more exposed to the water and thereby more effectively solvated. In this mode, the distance from tryptophan to the naphthalenic structures increases to 13.3 Å (Table 3). The polypyrrole portion of the PNU145156E, in between the two charged ends, interacts with the surface of the protein and through hydrophobic interactions causes the so-called "induced fit." This renders the protein more compact and water molecules are expelled from the interface of the hydrophobic surfaces. Based on time-resolved fluorescence anisotropy studies, we have found that PNU145156E at high concentrations, i.e., above 5 μM, aggregates up to decamers (data not shown). This occurs despite it being negatively charged, which points to the strong hydrophobic forces that dominate the formation of the aggregates. Accordingly, the interaction of PNU145156E with the doubly mutated bFGF, in which two positive charges have been eliminated, is primarily controlled by hydrophobic interactions.

The results of both CD (Fig. 7) and temperature stability (Fig. 8) measurements complemented the general picture emerging from the thermodynamic and kinetic findings, i.e., that the wild-type bFGF is destabilized upon binding to PNU145156E. The similarity between the CD spectrum of free bFGF at pH 9.5, which is the isoelectric point, and that obtained for the complex at pH 7.1, further supported this proposed destabilizing-denaturation effect. Neutralization of the positive charges on bFGF, be it by the negatively charged PNU145156E or by hydroxylic moieties at the basic pH, destabilizes the protein: free bFGF has a shape distinct from either β-sheet or α-helix, perhaps a signature of the compact three-dimensional β-barrel structure (Eriks-

son et al., 1993). Upon PNU145156E binding, destabilization of the β-barrel structure as bFGF approaches its isoelectric point (pH 9.5) is thus proposed. It is known that hydrophobic interactions in the cavity play an important role in maintaining bFGF overall structure (Ogura et al., 1999).

Similarly, PNU145156E binding resulted in ~10°C decrease in the thermal stability of bFGF. These suggested that binding of PNU145156E destabilizes the protein relative to the free protein, which is in contrast to the increase in stability of bFGF upon binding heparin. The binding to heparin induces conformational changes that extend well beyond its binding site and affects the whole structure of the protein. These changes cause a net decrease in the flexibility of the protein, which affects the regions on FGF that interact with the HARs (Lozano et al., 1998). The more compact structure obtained is thus suggested as a prerequisite for the binding of bFGF to the receptor. The binding to PNU145156E however, results in increased destabilization and flexibility of the protein, presumably adding to its reduced binding to the receptor. Similar observations have been recently reported using nuclear magnetic resonance studies of acidic-FGF (FGF-1) interaction with NTS, another heparin analog (Lozano et al., 1998).

CONCLUSIONS

In our study we distinguish between two different effects of the removal of charged polar amino acids. The first is the decrease in the binding constant and the resulting loosening of the complex, i.e., the complex turning less restricted in space, adopting a shallower energy minimal profile. The second is the effect induced by the drug upon protein folding, which, with reduced surface charge, becomes more compact and less flexible. In particular, the complex with the wild-type bFGF is tight although the protein is destabilized and turns more aqueously exposed and more flexible. The double mutant however, portrays the other extreme: a much weaker protein drug interaction is accompanied by a pronounced folding into a more compact protein structure. With heparin however, wild-type bFGF formed a tighter complex yet rendered bFGF more compact and stable. The partial denaturation induced by PNU145156E upon bFGF further contributes to blocking bFGF biological activity. This, together with PNU145156E blocking bFGF dimerization, renders this drug a potentially efficient antiangiogenic agent.

We thank Prof. Elisha Haas, from The Faculty of Life Sciences, Bar Ilan University, for the use of his single photon correlation spectrofluorometer. The help of D.E. Epps and R.W. Sarver from Discovery Technologies and Structural and Medicinal Chemistry, Pharmacia Corp. Kalamazoo MI 49001 is highly appreciated. We thank the Israeli Academy of Sciences, VATAT (no. 9027/98) for the purchase of the K-2 Multifrequency phase-modulation spectrofluorometer. This work was partially supported by the James Franck Center for Laser-Matter Interaction and by a grant (no. 81072101, 1999–2000) from the Vice-President of Research and Development, Ben-Gurion University of the Negev.

REFERENCES

Auerbach, W., and R. Auerbach. 1994. Angiogenesis inhibitors: a review. *Pharmac. Ther.* 63:265–311.

Baird, A., D. Schubert, N. Ling, and R. Guillemin. 1988. Receptor- and heparin-binding domains of basic fibroblast growth factor. *Proc. Natl. Acad. Sci. U.S.A.* 85:2324–2328.

Biasoli, G., M. Botta, M. Ciomei, F. Corelli, M. Grandi, F. Manetti, N. Mongelli, and A. Paio. 1993. New heterocyclic analogs of suramin with bFGF inhibiting activity: synthesis, sar and possible mode of action. *Med. Chem. Res.* 4:202–210.

Blood, C. H., and B. R. Zetter. 1990. Tumor interaction with the vasculature: angiogenesis and tumor metastasis. *Biochem. Biophys. Acta.* 1032:89–118.

Blumberg, W. E., R. E. Dale, J. Eisinger, and D. M. Zuckerman. 1974. Energy transfer in tRNAPhe (yeast): solution structure of transfer RNA. *Biopolymers.* 13:1607–1620.

Braddock, P. S., D. E., Hu., T. P. D., Fan, I. J., Stratford, A. L. Harris, and R. Bicknell. 1994. A structure-activity analysis of antagonism of the growth factor and angiogenic activity of basic fibroblast growth factor suramin and related polyanions. *Brit. J. Cancer.* 69:890–898.

Burgess, W. H., and T. Maciag. 1989. The heparin-binding (fibroblast) growth factor family of proteins. *Annu. Rev. Biochem.* 58:575–606.

Cantor, C. R., and P. R. Schimmel. 1980. *In* Biophysical Chemistry. W.H. Freeman and Company, New York. 995 and 1287.

Ciomei, M., W. Pastori, W. Mariani, F. Sola, M. Grandi, and N. Mongelli. 1993. New sulfonated distamycin A derivatives with bFGF complexing activity. *Biochem. Pharmacol.* 47:295–302.

Courtney, S. H., and G. R. Fleming. 1985. Photoisomerization of stilbene in low viscosity solvents: comparison of isolated and solvated molecules. *J. Chem. Phys.* 83:215–222.

Dale, R. E., J. Eisinger, and W. E. Blumberg. 1979. The orientational freedom of molecular probes: the orientation factor in intramolecular energy transfer. *Biophys. J.* 26:161–193.

Digabriele, A. D., I. Lax, D. I. Chen, C. M. Svahn, M. Jaye, J. Schlessinger, and W. A. Hendrickson. 1998. Structure of a heparin-linked biologically active dimer of fibroblast growth factor. *Nat. (Lond.).* 393:812–817.

Eriksson, A. E., L. S. Cousens, and B. W. Matthews. 1993. Refinement of the structure of human basic fibroblast growth factor at 1.6 Å resolution and analysis of presumed heparin binding sites by selenates substitution. *Prot. Sci.* 2:1274–1284.

Eriksson, A. E., L. S. Cousens, L. H. Weaver, and B. W. Matthews. 1991. Three-dimensional structure of human basic fibroblast growth factor. *Proc. Natl. Acad. Sci. U.S.A.* 88:3441–3445.

Faergeman, N. J., B. W. Sigurskjold, B. B. Kragelund, K. V. Andersen, and J. Knudsen. 1996. Thermodynamics of ligand binding to acyl-coenzyme A binding protein studied by titration calorimetry. *Biochemistry.* 35: 14118–14126.

Faham, S., R. E. Hileman, J. R. Fromm, R. J. Linhardt, and D. C. Rees. 1996. Heparin structure and interactions with basic fibroblast growth factor. *Science.* 271:1116–1120.

Fernig, D. G., and J. T. Gallagher. 1994. Fibroblast growth factors and their receptors: an information network controlling tissue growth, morphogenesis and repair. *Prog. Growth Factor Res.* 5:353–377.

Folkman, J. 1971. Tumor angiogenesis: therapeutic implications. *N. Engl. J. Med.* 285:1182–1186.

Folkman, J. 1985. Tumor angiogenesis. *Adv. Cancer Res.* 43:175–203.

Folkman, J., and M. Klagsbrun. 1987. Angiogeneic factors. *Science.* 235: 442–447.

Förster, Th. 1965. Delocalized excitation and excitation transfer. *In* Modern Quantum Chemistry, Part III. O. Sinanoglu, editor. Academic Press, Inc. New York. 93–137.

Gottfried, D. S., and E. Haas. 1992. Nonlocal interactions stabilize compact folding intermediates in reduced unfolded bovine pancreatic trypsin inhibitor. *Biochemistry.* 31:12353–12362.

Gullino, P. M. 1978. Angiogenesis and oncogenesis. *J. Natl. Cancer Inst.* 61:639–643.

Haas, E. 1996. The problem of protein folding and dynamics: time resolved dynamic non-radiative excitation energy transfer measurements. *IEEE J. Sel. Top. Quant.* 2:1088–1106.

Hansen, J. E., S. J. Rosenthal, and R. Fleming. 1992. Subpicosecond fluorescence depolarization studies of tryptophan and tryptophanyl residues of proteins. *J. Phys. Chem.* 96:3034–3040.

Herblin, W. F., S. Brem, T. P. Fan, and J. L. Gross. 1994. Recent advances in angiogenesis inhibitors. *Exp. Opin. Ther. Patents.* 6:641–654.

Herr, A. B., D. M. Ornitz, R. Sasisekharan, G. Venkataraman, and G. Waksman. 1997. Heparin-induced self-association of fibroblast growth factor-2: evidence for two oligomerization processes. *J. Biol. Chem.* 272:16382–16389.

Hulme, E. C., and N. J. M. Birdsall. 1992. Strategy and tactics in receptor-binding studies. *In* Receptor-Ligand Interactions. A Practical Approach. E. C. Hulme, editor. Oxford University Press, New York. 63–176.

Klagsbrun, M., and P. A. D'Amore. 1991. Regulators of angiogenesis. *Annu. Rev. Physiol.* 53:17–39.

Kohler, K., J. Trepel, and W. Linehan. 1992. Suramin: a novel growth factor antagonist with activity in hormone-refractory metastatic cancer. *J. Clin. Oncol.* 10:881–889.

La Rocca, R. V., C. A. Stein, and C. E. Meyers. 1990. Suramin: prototype of a new generation of antitumor compounds. *Cancer Cells.* 2:106–115.

Li, L. -Y., M. Safran, D. Aviezer, P. Bohlen, A. P. Seddon, and A. Yayon. 1994. Diminished heparin binding of a basic fibroblast growth factor mutant is associated with reduced receptor binding, mitogenesis, plasminogen activator induction, and in vitro angiogenesis. *Biochemistry.* 33:10999–11007.

Lindahl, U., K. Lidholt, D. Spillmann, and L. Kjellen. 1994. More to heparin than anticoagulation. *Thromb. Res.* 75:1–32.

Liotta, L. A., P. S. Steeg, and W. G. Stetler-Stevenson. 1991. Cancer metastasis and angiogenesis: an imbalance of positive and negative regulation. *Cell.* 64:327–336.

Lozano, R. M., M. A. Jimenez, J. Santoro, M. Rico, and G. Gimenez-Gallego. 1998. Solution structure of acidic fibroblast growth factor bound to 1,3,6-naphthalenetrissulfonate: a minimal model for the antitumoral action of suramins and suradistas. *J. Mol. Biol.* 281:899–915.

Manetti, F., V. Cappello, M. Botta, F. Corelli, N. Mongelli, G. Biasoli, A. L. Borgia, and M. Ciomei. 1998. Synthesis and binding mode of heterocyclic analogs of suramin inhibiting the human basic fibroblast growth factor. *Bioorg. Med. Chem.* 6:947–958.

Manetti, F., F. Corelli, and M. Botta. 2000. Fibroblast growth factors and their inhibitors. *Curr. Pharm. Design.* 6:1897–1924.

Middaugh, C. R., H. Mach, C. J. Burke, D. B. Volking, J. M. Dabora, P. K. Tsai, M. W. Bruner, J. A. Ryan, and K. E. Marfia. 1992. Nature of the interaction of growth factors with suramin. *Biochemistry.* 31: 9016–9024.

Ogura, K., K. Nagata, H. Hatanaka, H. Habuchi, K. Kimata, S. Tata, M. W. Ravera, M. Jaye, J. Schlessinger, and F. Inagaki. 1999. Solution structure of human acidic fibroblast growth factor and interaction with heparin-derived hexasaccharide. *J. Biomol. NMR.* 13:11–24.

Ornitz, D. M., A. B. Herr, M. Nilsson, J. Westman, C. M. Svahn, and G. Waksman. 1995. FGF binding and FGF receptor activation by synthetic heparan-derived di- and trisaccharides. *Science.* 268:432–436.

Pineda-Lucene, A., M. A. Jimenez, R. M. Lozano, J. L. Nieto, J. Santoro, M. Rico, and G. Gimenez-Gallego. 1998. Three-dimensional structure of acidic fibroblast growth factor in solution: effects of binding to a heparin functional analog. *J. Mol. Biol*. 284:162–178.

Plotnikov, A. N., J. Schlessinger, S. R. Hubbard, and M. Mohammadi. 1999. Structural basis for FGF receptor dimerization and activation. *Cell.* 98:641–650.

Presta, M., A. Rusnati, P. Gualandris, C. Dell'Era, D. Urbinati, E. Coltrini, S. Tanghetti, and M. Belleri. 1994. Human basic fibroblast growth factor: structure-function relationship of an angiogeneic molecule. *In* Angiogenesis: Molecular Biology, Clinical Aspects, Series A: Life Sciences, Vol. 263. M. E. Maragoudakis, P. M. Gullino, and P. I. Lelkes, editors. Plenum Press, New York. 39–50.

Sola, F., L. Capolongo, D. Moneta, P. Ubezio, and M. Grandi. 1999. The antitumor efficacy of cytotoxic drugs is potentiated by treatment with PNU 145156E, a growth factor complexing molecule. *Cancer Chemother. Pharmacol.* 43:241–246.

Sola, F., M. Farao, E. Pesenti, A. Marsilio, N. Mongelli, and M. Grandi. 1995. Antitumoral activity of FCE26644 a new growth-factor complexing molecule. *Cancer Chemother. Pharmacol.* 36:217–222.

Spolar, R. S., and T. M. Record, Jr. 1994. Coupling of local folding to site-specific binding of proteins to DNA. *Science*. 263:777–784.

Springer, B. A., M. W. Pantoliano, F. A. Barbera, P. L. Gunyuzlu, L. D. Thompson, W. F. Herblin, S. A. Rosenfeld, and G. W. Book. 1994. Identification and concerted function of two receptor-binding surfaces on basic fibroblast growth factor required for mitogenesis. *J. Biol. Chem.* 269:26869–26884.

Thompson, L. D., M. W. Pantoliano, and B. A. Springer. 1994. Energetic characterization of the basic fibroblast growth factor-heparin interaction: identification of the heparin binding domain. *Biochemistry.* 33: 3831–3840.

Venkataraman, G., V. Sasisekaharan, A. B. Herr, D. M. Ornitz, G. Waksman, C. L. Cooney, R. Langer, and R. Sasisekharan. 1996. Preferential self-association of basic fibroblast growth factor is stabilized by heparin during receptor dimerization and activation. *Proc. Natl. Acad. Sci. U.S.A.* 93:845–850.

Waksman, G., and A. B. Herr. 1998. New insights into heparin-induced FGF oligomerization. *Nat. Struct. Biol.* 5:527–530.

Yayon, A., M. Klagsbrun, J. D. Esko, P. Leder, and D. M. Ornitz. 1991. Cell surface, heparin-like molecules are required for binding of basic fibroblast growth factor to its high affinity receptor. *Cell.* 64:841–848.

Zamai. M., V. R. Caiolfa, D. Pines, E. Pines, and A. H. Parola. 1998. Nature of interaction between basic fibroblast growth factor and the antiangiogenic drug 7,7-(carbonyl-bis-[imino-*N*-methyl-4,2-pyrrolecarbonylimino[*N*-methyl-4,2-pyrrole]-carbonylimino])-bis-(1,3-naphthalene disulfonate). *Biophys. J.* 75:672–682.

Zamai, M., A. H. Parola, N. Mongelli, M. Grandi, and V. R. Caiolfa. 1997. Antiangiogenic naphthalene sulfonic distamycin-A derivatives tightly interact with human basic fibroblast growth factor. *Med. Chem. Res.* 7:36–44.

Zhu, H., K. Ramnarayan, J. Anchin, W. Y. Miao, A. Sereno, L. Millman, J. Zheng, V. N. Balaji, and M. E. Wolff. 1995. Glu-96 of basic fibroblast growth factor is essential for high affinity receptor binding. *J. Biol. Chem.* 270:21869–21874.

Zhu, X., H. Komiya, A. Chirino, S. Faham, G. M. Fox, T. Arakawa, B. T. Hsu, and D. C. Rees. 1990. Three-dimensional structure of acidic and basic fibroblast growth factors. *Science.* 251:90–93.